JACS
JOURNAL OF THE AMERICAN CHEMICAL SOCIETY

Communication

pubs.acs.org/JACS

Metal–Organic Nanotube with Helical and Propeller-Chiral Motifs Composed of a C_{10}-Symmetric Double-Decker Nanoring

Hiroshi Yamagishi,[†] Takahiro Fukino,*[,†] Daisuke Hashizume,[‡] Tadashi Mori,[§] Yoshihisa Inoue,[§] Takaaki Hikima,[∥] Masaki Takata,[∥] and Takuzo Aida*[,†,‡]

[†]Department of Chemistry and Biotechnology, School of Engineering, The University of Tokyo, 7-3-1 Hongo, Bunkyo-ku, Tokyo 113-8656, Japan

[‡]RIKEN Center for Emergent Matter Science, 2-1 Hirosawa, Wako, Saitama 351-0198, Japan

[§]Department of Applied Chemistry, Graduate School of Engineering, Osaka University, 2-1 Yamada-oka, Suita, Osaka 565-0871, Japan

[∥]RIKEN SPring-8 Center, 1-1-1 Kouto, Sayo, Hyogo 679-5198, Japan

Supporting Information

ABSTRACT: Coassembly of an achiral ferrocene-cored tetratopic pyridyl ligand (**FcL**) with $AgBF_4$ in CH_2Cl_2/MeCN (7:3 v/v) containing chiral Bu_4N^+ (+)- or (−)-menthylsulfate (MS^{*-}) results in the formation of an "optically active" metal–organic nanotube (**FcNT**) composed of a C_{10}-symmetric double-decker nanoring featuring 10 **FcL** units and 20 Ag^+ ions. The circular dichroism spectrum of **FcNT** along with its 2D X-ray diffraction (2D XRD) pattern indicates that the constituent metal–organic nanorings in **FcNT** stack one-handed helically on top of each other. A crystal structure of the dimeric double-decker model complex (Ag_2(**FcL′**)$_2$) from a ditopic ferrocene ligand (**FcL′**) and $AgBF_4$ allowed for confirming the binding of MS^{*-} onto the Ag^+ center of the complex. The results of detailed spectroscopic studies indicate that in its double-decker aromatic arrays, **FcNT** possibly possesses propeller-chiral twists in addition to the helically chiral structure, where the former is considerably more dynamic than the latter. Notably, both chiral structural motifs responded nonlinearly to an enantiomeric excess of MS^{*-} (majority rule) though with no stereochemical influence on one another.

Helices exhibit beautiful structural motifs that have been utilized for many historical architectures. In the mid 1970s, some synthetic polymers were found to adopt a helical geometry in solution,[1] and currently, a wide variety of helical polymers including noncovalent helical assemblies are known.[2,3] Helical nanotubes are one of the most complicated classes of helical polymers since nanotubes are categorized into 1D architectures morphologically but composed of a rolled up 2D sheet. A successful synthetic strategy toward helical nanotubes would be to stack polygonal macrocycles on top of each other in a one-handed helical manner. Although successful examples of this strategy have been reported, they are only limited to the helical stacking of C_2-, C_3-, C_4-, and C_6-symmetric macrocycles.[4] Herein, we report a new nanotubular assembly that is uniquely composed of a C_{10}-symmetric ultralarge coordination nanoring. Note that helical stacking of C_{10}-symmetric macrocycles is far more difficult than that of lower-symmetry examples because the stacked nanorings must be twisted unidirectionally with a regular twisting angle of less than 18° (Figure 1b). Therefore, elaboration of the self-assembly is required.

In a previous study,[5] we reported that a ferrocene-cored tetratopic pyridyl ligand (**FcL**) and $AgBF_4$ coassemble in MeCN to afford a metal–organic nanotube (**FcNT**). Although this nanotubular coassembly occurs stochastically, **FcNT** is composed of a large number of decagonal nanorings with a diameter of 7.5 nm (Figure 1a), which is unusually large and has been out of range for direct synthesis using conventional coordination chemistry. In **FcNT**, the decagonal nanorings are stacked via π–electronic interactions. If they stack normally on top of each other, metallophilic (Ag–Ag) interactions among the stacked nanorings can also be expected. We initially thought that this normal stacking is the most likely candidate. However, a closer examination of the 2D X-ray diffraction (2D XRD) image of the magnetically oriented **FcNT**s indicated that a small helical twist may exist in the stacking geometry.[6] If this helical twist can unidirectionally be developed over the entire nanotube, **FcNT** would be optically active. As described below, when the coassembly was carried out in the presence of (+)- or (−)-menthylsulfate (MS^{*-}), the resultant nanotube indeed displayed an optical activity.

Figure 2a shows a 2D XRD image of magnetically oriented **FcNT**s prepared under a 10 T magnetic field by slow solvent evaporation of an MeCN dispersion of a mixture of $Bu_4N^+OTf^-$ (8 mM) and **FcNT**, formed from **FcL** (4 mM) and $AgBF_4$ (8 mM) at 25 °C. In addition to meridional and equatorial diffractions due to the intra- and intercolumnar orderings, respectively, of **FcNT**, two sets of four-split diffraction spots were observed at q = 3.6 (red arrows) and 6.9 nm^{-1} (blue arrows). Although the diffraction maxima were blurred, azimuthal plots at the q values in Figure 2c,e indicated the existence of two sets of four-split diffractions characteristic of the helical twists.[6] Simulation of the 2D XRD pattern of **FcNT** (Figure 2a) using the HELIX[7] program provided a simple atomistic model with a probable twisting angle of 4° (Figure S7).[8] If this twisting results

Received: April 28, 2015
Published: June 8, 2015

DOI: 10.1021/jacs.5b04386
J. Am. Chem. Soc. 2015, 137, 7628–7631

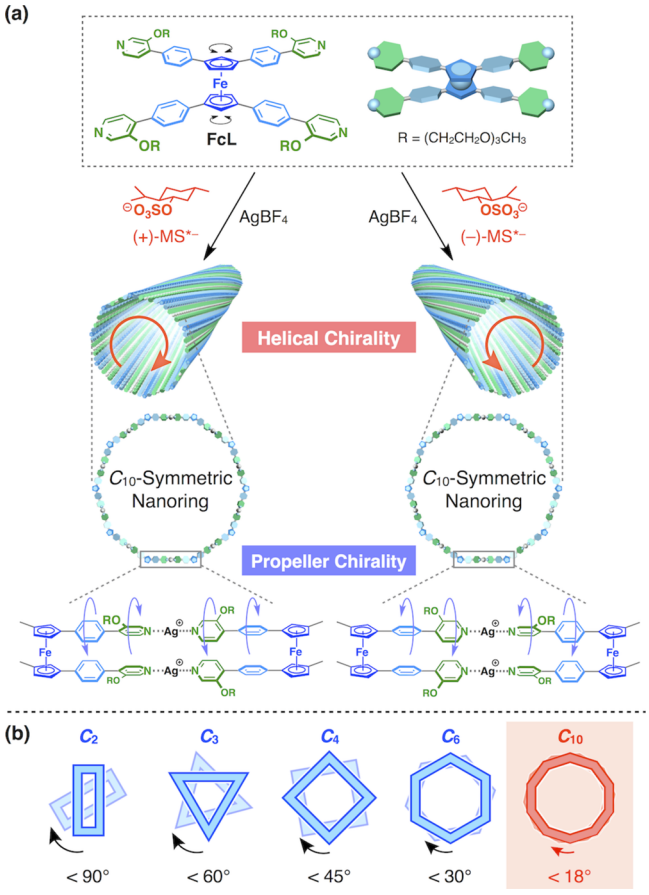

Figure 1. (a) Schematic representations of the coassembly of ferrocene-cored tetratopic pyridyl ligand (**FcL**) and $AgBF_4$ in the presence of (+)- or (−)-menthylsulfate (MS^{*-}), and possible helical and propeller-chiral motifs in the resulting helical metal−organic nanotube (**FcNT**). (b) Upper-limit rotational angles for achieving the helical stacking of the C_2-, C_3-, C_4-, C_6-, and C_{10}-symmetric macrocycles.[4]

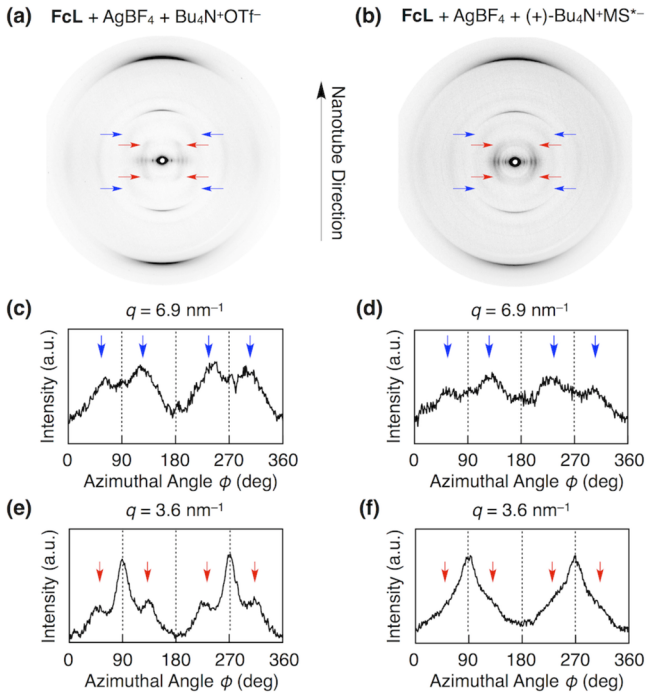

Figure 2. Two-dimensional X-ray diffraction (2D XRD) patterns of film samples of magnetically oriented **FcNT**s carrying (a) OTf^- prepared from **FcL** (4 mM), $AgBF_4$ (8 mM), and $Bu_4N^+OTf^-$ (8 mM), and (b) MS^{*-} prepared from **FcL** (2 mM), $AgBF_4$ (4 mM), and (+)-$Bu_4N^+MS^{*-}$ (4 mM) in MeCN. Azimuthal plots for the (a,b) 2D XRD intensities at q = (c,d) 6.9 and (e,f) 3.6 nm^{-1} as a function of the azimuthal angle (ϕ). Red and blue arrows indicate that the diffraction spots split into four-spot patterns.

in a single-handed helix, a helical pitch of ca. 64 nm is expected. An analogous XRD pattern was observed for **FcNT** with (+)-$Bu_4N^+MS^{*-}$ (Figure 2b,d,f), indicating that **FcNT** is intrinsically composed of helical twists, regardless of whether **FcNT** carries chiral counterions or not.

Prior to detailed studies of **FcNT**, we attempted to synthesize a dimeric complex (Ag_2(**FcL′**)$_2$) as a model for the double-decker constituent of **FcNT**. Therefore, a ditopic ferrocene ligand (**FcL′**) bearing only two pyridyl groups (4 mM) was coassembled with $AgBF_4$ (4 mM) in the presence of (+)-$Bu_4N^+MS^{*-}$ (4 mM) in THF/MeCN (99.5:0.5 v/v) (Figure 3a).[8] When cyclohexane vapor was allowed to diffuse slowly at 25 °C into this coassembling mixture, a single crystal appropriate for X-ray crystallography was formed. The crystal adopted a chiral space group of $P2_12_12_1$ with a composition of Ag_2(**FcL′**)$_2$(BF_4)-((+)-MS^{*-})(THF), as determined by elemental analysis.[8] The ORTEP diagram in Figure 3b indicates that two **FcL′** molecules adopt an eclipsed geometry and are ditopically connected by Ag^+ ions to form a double-decker structure. This structure is consistent with the building unit for **FcNT** proposed in our previous study.[5] Notably, a bulky (+)-MS^{*-} anion is located on one side of Ag_2(**FcL′**)$_2$ and its sulfate group bridges two Ag^+ atoms. In addition, a BF_4^- anion is located on the other side of the double-decker structure. The crystal packing diagram of Ag_2(**FcL′**)$_2$ (Figure 3c) indicates that Ag_2(**FcL′**)$_2$ stacks on top of each other due to π−electronic interactions.

As a typical example of nanotubular coassembly, a CH_2Cl_2/MeCN (7:3 v/v) solution consisting of a mixture of **FcL** (100 μM), $AgBF_4$ (200 μM), and (+)-$Bu_4N^+MS^{*-}$ (200 μM) was allowed to stand at 25 °C for 12 h without stirring. Then, a transparent orange dispersion resulted. As shown in Figure 4a, this dispersion exhibited an intense absorption band at 335 nm (solid curve), which was red-shifted from that of nonassembled **FcL** at 307 nm (broken curve) due to the π−π^* transition of its π-conjugated arms. Transmission electron microscopy (TEM; Figure 4b) and atomic force microscopy (AFM; Figure S6) studies of its air-dried residue indicated the formation of hollow cylinders with a uniform diameter of 7.3 nm. When $Bu_4N^+MS^{*-}$ was mixed with **FcNT** ($[MS^{*-}]/[Ag^+]$ = 1.0) in CD_3CN, ^1H NMR signals due to MS^{*-} disappeared, but those due to Bu_4N^+ remained unchanged (Figure S5), indicating that MS^{*-} is tightly bound to Ag^+ (see also Figure 3b).[9] **FcNT**, which formed in the presence of (+)- or (−)-MS^{*-}, was optically active and exhibited Cotton effects at 325 and 343 nm in its circular dichroism (CD) spectrum (Figure 4c). This result is exciting because **FcNT** is composed of a C_{10}-symmetric nanoring and can be optically active only when the twisting angle of the stacked nanorings is less than 18°. The CD spectrum of **FcNT** with (+)-MS^{*-} was a mirror-image of that with (−)-MS^{*-}.

Next, the dynamic nature of this unique helical nanotube was investigated. First, **FcNT** was prepared in the presence of (+)-$Bu_4N^+MS^{*-}$ (200 μM) in CH_2Cl_2/MeCN (7:3 v/v) under ordinary conditions, and an excess amount of (−)-$Bu_4N^+MS^{*-}$ (600 μM) was added to the resulting dispersion. Interestingly,

DOI: 10.1021/jacs.5b04386
J. Am. Chem. Soc. 2015, 137, 7628−7631

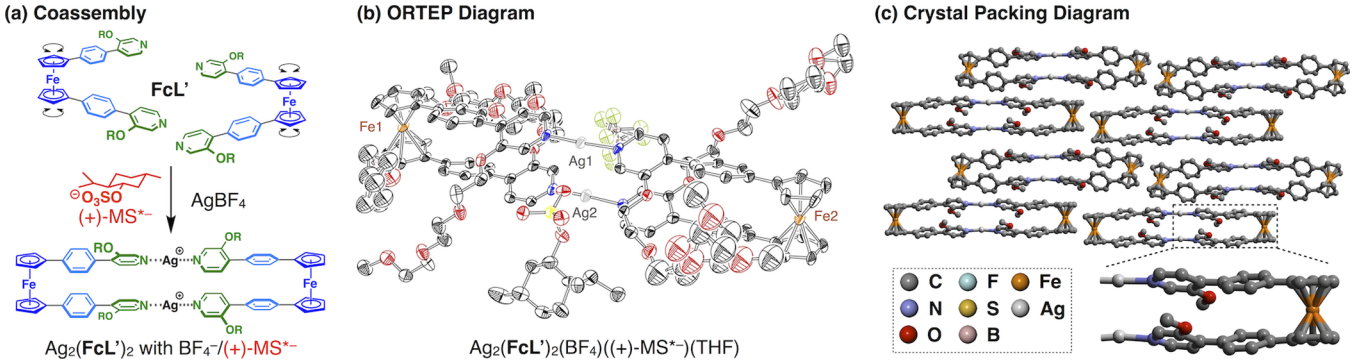

Figure 3. (a) Schematic representation of the coassembly of **FcL**′ with $AgBF_4$ in the presence of (+)-$Bu_4N^+MS^{*-}$. (b) An ORTEP diagram of the $Ag_2(\mathbf{FcL}')_2(BF_4)((+)\text{-}MS^{*-})(THF)$ dimeric complex with a probability level of 30%. Three of the four triethylene glycol (TEG) chains, BF_4^-, and a THF molecule are disordered. (c) A crystal packing diagram of $Ag_2(\mathbf{FcL}')_2(BF_4)((+)\text{-}MS^{*-})(THF)$ with a magnified image of the aromatic rings of **FcL**′. The TEG chains, BF_4^-, MS^{*-}, and a THF molecule are omitted for clarity.

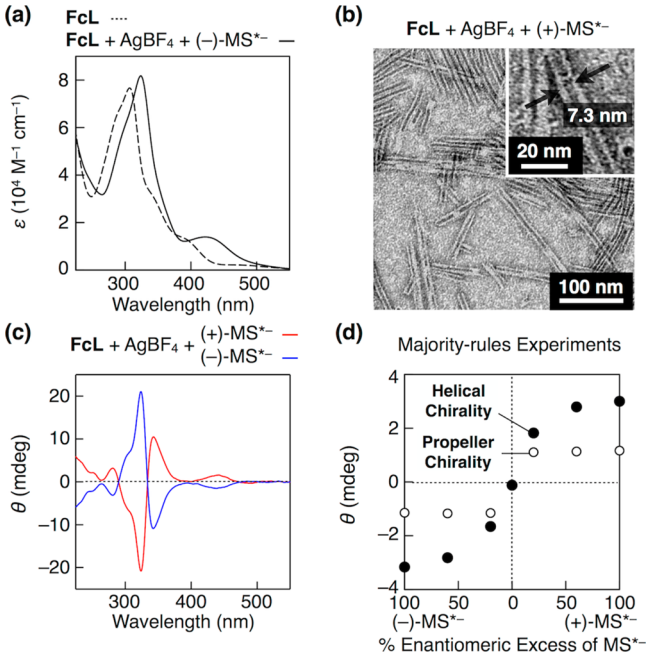

Figure 4. Coassembly of **FcL** (100 μM) with $AgBF_4$ (200 μM) at 25 °C in CH_2Cl_2/MeCN (7:3 v/v) containing (+)- or (−)-$Bu_4N^+MS^{*-}$ (200 μM). (a) Electronic absorption spectra of **FcNT** prepared in the presence of (−)-$Bu_4N^+MS^{*-}$ (solid curve) and **FcL** alone (100 μM; broken curve) as a reference in a 1.0 mm-thick quartz cell. (b) A TEM image of an air-dried sample of **FcNT** prepared in the presence of (+)-$Bu_4N^+MS^{*-}$ and stained with uranyl acetate. Inset shows a magnified TEM image. (c) CD spectra of **FcNT** assembled in the presence of (+)- (red curve) and (−)-$Bu_4N^+MS^{*-}$ (blue curve) in a 1.0 mm-thick quartz cell. (d) Changes in the θ values at 278 (○) and 352 nm (●) as a function of the % enantiomeric excess (%*ee*) of MS^{*-}.

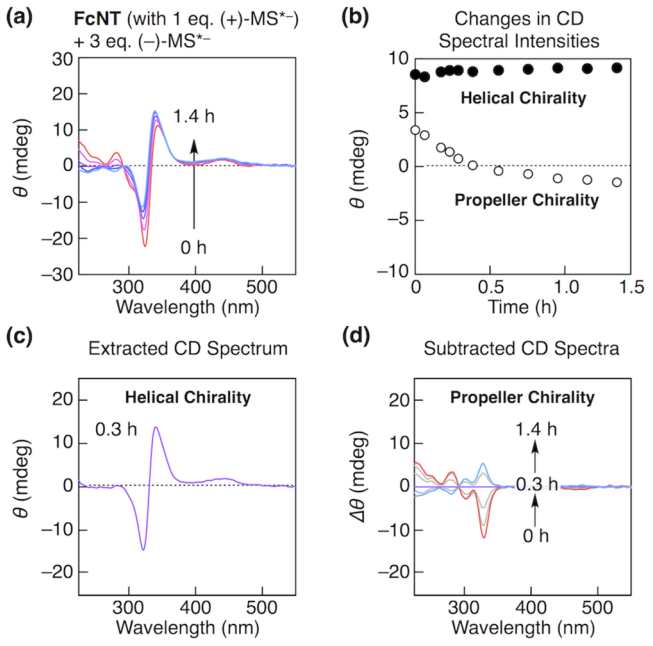

Figure 5. Addition of (−)-$Bu_4N^+MS^{*-}$ to a dispersion of **FcNT** ($[(-)\text{-}MS^{*-}]/[Ag^+]$ = 3.0) in CH_2Cl_2/MeCN (7:3 v/v), prepared by the coassembly of **FcL** (100 μM) with $AgBF_4$ (200 μM) at 25 °C in the presence of (+)-$Bu_4N^+MS^{*-}$ (200 μM). (a) Time-dependent CD spectral change after the addition of (−)-$Bu_4N^+MS^{*-}$. (b) Plots of the CD spectral intensities at 278 (○) and 352 nm (●) due to the propeller-chiral and helical geometries, respectively. (c) A CD spectrum extracted from panel a, which was observed in 0.3 h upon addition of (−)-$Bu_4N^+MS^{*-}$. (d) Calculated CD spectra obtained by subtraction of the CD spectrum in panel c from those in panel a.

minor CD bands corresponding to **FcNT** at 240−290 nm underwent inversion, whereas the residual major bands remained virtually intact (Figure 5a), suggesting that **FcNT** contains two chiral structural motifs with different dynamic properties. The minor CD bands only disappeared in 0.3 h (Figure 5c). Therefore, a split Cotton effect, which is characteristic of helical motifs,[10] was observed with positively and negatively signed CD bands at 340 and 322 nm, respectively (Figure 5c). As discussed later, this CD activity is long-lived. The dynamic CD components were extracted (Figure 5d) by subtracting this particular spectrum from the CD spectra in Figure 5a. We assume that the domino-like condensed aromatic arrays in **FcNT** adopt a propeller-chiral geometry (Figure 1a), which results in these dynamic CD bands. Based on a closer examination of the structure of $Ag_2(\mathbf{FcL}')_2$ in Figure 3c, the phenyl and pyridyl rings in **FcL**′ are tilted in opposite directions by +17 and −21° (or −17 and +21°), respectively, relative to the Cp rings in the proximal ferrocene unit. Such propeller-chiral structures are well-known for *ortho*-substituted biaryls.[11] Time-dependent DFT calculations based on a dimeric model complex with an energy-minimized geometry (Figure S8) provided a simulated CD spectrum (Figure S9), which is consistent with the one observed for $Ag_2(\mathbf{FcL}')_2$ in THF at −80 °C.[8] As described above, by comparison with the CD spectral change for the propeller-chiral

DOI: 10.1021/jacs.5b04386
J. Am. Chem. Soc. 2015, 137, 7628−7631

structure (Figure 5b, open circles) in **FcNT**, the change due to the helical structure was much more sluggish (Figure 5b, filled circles), where only 14% CD attenuation at 352 nm occurred in 6.9 h.

In Figure 4d, (+)- and (−)-$Bu_4N^+MS^{*-}$, mixed at varying mole ratios, were employed for the formation of **FcNT**, where the CD intensities at 278 (open circles; propeller chirality) and 352 nm (filled circles; helical chirality) both changed sigmoidally with the % enantiomeric excess (%*ee*) of MS^{*-}. Therefore, the two different chiral motifs in **FcNT** (Figure 1a) follow the majority rule.[12] Note that the aromatic units in **FcNT**, adopting a propeller-chiral geometry, are sterically congested, so that their conformational changes may not be free from one another but synchronous like a "domino".[13] The sigmoidal response of the helical chirality to the %*ee* of MS^{*-} may also be reasonable, considering that each nanoring can accommodate 20 chiral anions, which must determine the twisting direction of the nanoring based on their majority voting. Of interest, the propeller and helical geometries in **FcNT** show different nonlinear responses to the %*ee* of MS^{*-} (Figure 4d). So, they do not influence on one another.

In conclusion, the nanotubular coassembly between achiral tetratopic pyridyl ligand **FcL** and $AgBF_4$ in the presence of a chiral Bu_4N^+ salt of (+)- or (−)-menthylsulfate (MS^{*-}) (Figure 1a) resulted in the formation of a metal−organic nanotube (**FcNT**) in an optically active form due to the successful stereochemical bias of the helical twist in the stacking geometry of the constituent nanorings in either a left- or right-handed manner. This achievement is noteworthy because the nanoring is highly symmetric (C_{10}-symmetric; Figure 1b) and needs fine-tuning in its stacking geometry to generate a one-handed helical twist. In addition to this helical chirality, **FcNT** possesses the propeller chirality (Figure 1a). Although both chiral motifs exhibit a nonlinear response to the %*ee* of the chiral auxiliary (MS^{*-}), their dynamic natures are different. The propeller-chiral motif is dynamic, whereas the helical motif is considerably less dynamic. Application of this unique chiral metal−organic nanotube for enantioselective catalysis and separation provides important areas for future investigation.

■ ASSOCIATED CONTENT

Supporting Information

Details of synthesis and characterization of **FcL′** and (+)-/(−)-$Bu_4N^+MS^{*-}$, analytical data by NMR, CD spectroscopy, atomic force microscopy, 2D XRD, and X-ray crystallography; and results of DFT calculations. The Supporting Information is available free of charge on the ACS Publications website at DOI: 10.1021/jacs.5b04386.

■ AUTHOR INFORMATION

Corresponding Authors

*fukino@macro.t.u-tokyo.ac.jp
*aida@macro.t.u-tokyo.ac.jp

Notes

The authors declare no competing financial interest.

■ ACKNOWLEDGMENTS

This work was supported by the Japan Society for the Promotion of Science (JSPS) through its Grant-in-Aid for Specially Promoted Research (25000005) on "Physically Perturbed Assembly for Tailoring High-Performance Soft Materials with Controlled Macroscopic Structural Anisotropy". H.Y. thanks JSPS for Leading Graduate Schools (MERIT) and Young Scientist Fellowship (27·8006). Synchrotron radiation experiments were performed at BL45XU[14] in SPring-8 with the approval of RIKEN SPring-8 Center (proposal 20130079).

■ REFERENCES

(1) (a) Nolte, R. J. M.; van Beijnen, A. J. M.; Drenth, W. *J. Am. Chem. Soc.* **1974**, *96*, 5932. (b) Okamoto, Y.; Suzuki, K.; Ohta, K.; Hatada, K.; Yuki, H. *J. Am. Chem. Soc.* **1979**, *101*, 4763.

(2) (a) Yashima, E.; Maeda, K.; Iida, H.; Furusho, Y.; Nagai, K. *Chem. Rev.* **2009**, *109*, 6102. (b) Schwartz, E.; Koepf, M.; Kitto, H. J.; Nolte, R. J. M.; Rowan, A. E. *Polym. Chem.* **2011**, *2*, 33.

(3) (a) Lee, C. C.; Grenier, C.; Meijer, E. W.; Schenning, A. P. H. J. *Chem. Soc. Rev.* **2009**, *38*, 671. (b) Pijper, D.; Feringa, B. L. *Soft Matter* **2008**, *4*, 1349.

(4) (a) Kim, H.-J.; Zin, W.-C.; Lee, M. *J. Am. Chem. Soc.* **2004**, *126*, 7009. (b) Liu, Z.; Liu, G.; Wu, Y.; Cao, D.; Sun, J.; Schneebeli, S. T.; Nassar, M. S.; Mirkin, C. A.; Stoddart, J. F. *J. Am. Chem. Soc.* **2014**, *136*, 16651. (c) Mariani, P.; Mazabard, C.; Garbesi, A.; Spada, G. P. *J. Am. Chem. Soc.* **1989**, *111*, 6369. (d) Fenniri, H.; Deng, B.-L.; Ribbe, A. E. *J. Am. Chem. Soc.* **2002**, *124*, 11064.

(5) Fukino, T.; Joo, H.; Hisada, Y.; Obana, M.; Yamagishi, H.; Hikima, T.; Takata, M.; Fujita, N.; Aida, T. *Science* **2014**, *344*, 499.

(6) (a) Peterca, M.; Imam, M. R.; Ahn, C.-H.; Balagurusamy, V. S. K.; Wilson, D. A.; Rosen, B. M.; Percec, V. *J. Am. Chem. Soc.* **2011**, *133*, 2311. (b) van Houtem, M. H. C. J.; Martín-Rapún, R.; Vekemans, J. A. J. M.; Meijer, E. W. *Chem.—Eur. J.* **2010**, *16*, 2258. (c) Jin, W.; Yamamoto, Y.; Fukushima, T.; Ishii, N.; Kim, J.; Kato, K.; Takata, M.; Aida, T. *J. Am. Chem. Soc.* **2008**, *130*, 9434.

(7) Knupp, C.; Squire, J. M. *J. Appl. Crystallogr.* **2004**, *37*, 832.

(8) See Supporting Information.

(9) (a) Escuder, B.; LLusar, M.; Miravet, J. F. *J. Org. Chem.* **2006**, *71*, 7747. (b) Yu, G.; Yan, X.; Han, C.; Huang, F. *Chem. Soc. Rev.* **2013**, *42*, 6697.

(10) (a) Berova, N.; Nakanishi, K.; Woody, R. W. *Circular Dichroism*, 2nd ed.; John Wiley & Sons, Inc.: New York, 2000. (b) Pescitelli, G.; Di Bari, L.; Berova, N. *Chem. Soc. Rev.* **2014**, *43*, 5211.

(11) Grein, F. *J. Phys. Chem. A* **2002**, *106*, 3823.

(12) (a) van Gestel, J.; Palmans, A. R. A.; Titulaer, B.; Vekemans, J. A. J. M.; Meijer, E. W. *J. Am. Chem. Soc.* **2005**, *127*, 5490. (b) Jin, W.; Fukushima, T.; Niki, M.; Kosaka, A.; Ishii, N.; Aida, T. *Proc. Natl. Acad. Sci. U.S.A.* **2005**, *102*, 10801. (c) Palmans, A. R. A.; Meijer, E. W. *Angew. Chem., Int. Ed.* **2007**, *46*, 8948.

(13) (a) Tang, H.-Z.; Novak, B. M.; He, J.; Polavarapu, P. L. *Angew. Chem., Int. Ed.* **2005**, *44*, 7298. (b) Merten, C.; Reuther, J. F.; DeSousa, J. D.; Novak, B. M. *Phys. Chem. Chem. Phys.* **2014**, *16*, 11456.

(14) Fujisawa, T.; Inoue, K.; Oka, T.; Iwamoto, H.; Uruga, T.; Kumasaka, T.; Inoko, Y.; Yagi, N.; Yamamoto, M.; Ueki, T. *J. Appl. Crystallogr.* **2000**, *33*, 797.

■ NOTE ADDED AFTER ASAP PUBLICATION

Figure 4 was corrected on June 16, 2015.

DOI: 10.1021/jacs.5b04386
J. Am. Chem. Soc. 2015, 137, 7628−7631